Theoretical Study of Vibrational and Optical Spectra of Methylene-Bridged Oligofluorenes

Vladimír Lukeš,*,† Adelia Aquino,‡ and Hans Lischka‡

Department of Chemical Physics, Slovak University of Technology, Radlinského 9, SK-81 237 Bratislava, Slovakia, and Institute for Theoretical Chemistry, University of Vienna, Währingerstrasse 17, A-1090 Wien, Austria

Received: August 1, 2005; In Final Form: September 15, 2005

We report a systematic characterization of methylene-bridged fluorene oligomers constructed of two, four, six, and eight aromatic rings using time-dependent density functional theory (TDDFT), the ab initio approximate coupled-cluster singles and doubles (CC2) method, and semiempirical spectroscopic Zerner's intermediate neglect of differential overlap method (ZINDO/S). Geometry optimizations have been performed for the ground state and for the first electronically excited state. Vertical excitations and the fluorescence transition from the lowest excited state have been calculated. Computed ground-state geometries and infrared spectra for fluorene are in good agreement with experimental results. The RI-CC2 and ZINDO/S absorption and fluorescence spectra agree very well with the available experimental data for studied fluorene oligomers and for para oligophenylenes films. On the other hand, TDDFT calculations underestimate excitation and fluorescence energies systematically for larger systems ($N > 4$) in comparison with the above-mentioned results. The effective conjugation length was estimated to 13−14 repeat units. The computed radiative lifetimes for the fluorene molecule show good agreement with experiment within realistic expectations. The decrease of the radiatiave fluorescence lifetime with the increase in the conjugation length has been discussed also.

1. Introduction

Phenyl-based conjugated polymers and oligomers are widely studied in view of their usage in electronic devices such as light-emitting diodes, solar cells, or field-effect transistors.[1−4] Whereas the polymeric structures are obtained as highly amorphous materials, their oligomers are of particular interest due to their relatively well-defined structure and easier manipulation, e.g., in terms of solubility, purification, and film preparation.[5,6]

One prospective way of preparation of novel molecules with the required photophysical properties is the modification of molecular structures using bridges or side chains. These enable the variation of the flexibility and electronic conjugation over the whole molecule. The rigid structure suppresses nonradiative deactivation pathways leading to high photoluminescence quantum yields and increases the effective conjugation due to the planarization of the π system. In contrast thereto, torsions between adjacent biphenyl moieties lead to strong conformational changes between the ground state and the lowest excited singlet states and keep the Stokes shift large.[7] The incorporation of CH_2 linkages between the phenylene rings in side positions represents a good possibility for a desired setting of dihedral angles between the aromatic rings.[5,8] The connection between adjacent rings (a simple example is fluorene) enforces the planarity of the carbon skeleton. Under these aspects, the family of fluorene oligomers has been investigated intensively with respect to synthesis and characterization by optical measurements.[9−19]

One major aim of theoretical investigations is the identification of relations between physical properties and molecular structure, which is the key tool for a rational design of new electronic fabrics and tuning of their photoelectronic properties.[1,5] The theoretical characterization of fluorene oligomer structures and optical spectra was presented so far only for the fluorene molecule[20] itself. The reason for this restriction is to be seen in the large size of these compounds and in the fact that the calculation of electronically excited states is still a very challenging task, especially if one wants to go beyond vertical excitations and compute geometry relaxation effects in excited states. In recent years, considerable progress has been made in the field of efficient calculation of excited states (see below) capable of accurately treating oligomer sizes of conjugated π systems large enough in order to be of relevance for predictions and discussions of realistic examples. One purpose of this paper was to apply these methods to fluorene oligomers, concentrating on electronically excited states in order to obtain new results in particular for excited-state geometries. Despite the just-mentioned progress in quantum chemical methods, their application to larger oligomer systems is far from being straightforward. Therefore, our second goal was the investigation of the reliability of these methods and the molecular sizes, which could be treated with standard present-day computational facilities. The assessment of the reliability of quantum chemical methods for oligomer/polymer calculations is difficult most of all because of the aforementioned size of the systems. The second problem is the fact that the calculations are usually performed for isolated systems and the experiments refer to solution or to the solid state. Moreover, the measured absorption or fluorescence band systems are usually not well resolved and experimentally determined excited-state geometries are not available for the classes of systems investigated here. Our goal is to obtain internal consistency of the calculated results in terms of basis set effects and to compare results obtained with different methods. Environmental effects will be discussed only in a very

* To whom correspondence should be addressed. E-mail: vladimir.lukes@stuba.sk.
† Slovak University of Technology.
‡ University of Vienna.

10.1021/jp054248s CCC: $30.25
Published on Web 10/25/2005

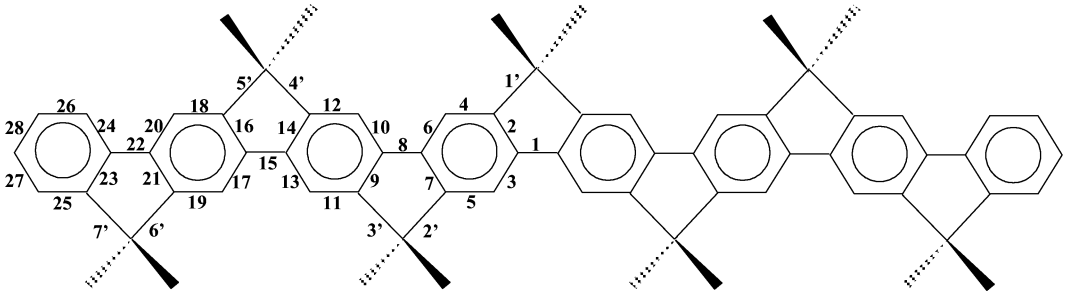

Figure 1. Structure and numbering scheme of fluorene-based oligomers with eight aromatic rings as example.

simple way by comparison of our gas-phase results with different experimental data.

By consideration of the size of the oligomers to be treated in this work, conceptually simple and cost-effective methods have to be used. One of the most popular methods is certainly the density functional (DFT) approach and its time-dependent (TD) extension for excited states. Major methodological progress has been achieved by the variational formulation of the TDDFT method by Furche and Ahlrichs[21] facilitating the calculation of analytic TDDFT gradients and thus allowing geometry optimizations in excited states. Despite the overwhelming success of DFT, one should not forget its shortcomings, which led to the development of a large number of functionals. The approximate coupled-cluster singles and doubles method (CC2)[22] is a very interesting alternative. The recent introduction of linear response theory in combination with analytic gradients[23] provides the required possibilities for the treatment of excited states. The implementation of the resolution of the identity (RI) method[24] allows the efficient treatment of larger molecules. Recently, it has been used successfully for the investigation of excited-state proton-transfer processes.[25] In addition to ab initio and DFT calculations, semiempirical methods are of great interest also. We chose the ZINDO/S method because of its great success for the calculation of excitation and fluorescence spectra. Unfortunately, with ZINDO/S, only vertical excitations can be calculated, so that geometries have to be obtained from other calculations.

In this work, we will focus our attention to indenofluorene oligomers containing 2, 4, 6, and 8 phenylene rings (see Figure 1). In the spirit of the description of different quantum chemical methods given above, we will use the DFT and RI-CC2 methods for the calculation of optimized electronic ground-state and lowest-excited geometries and vibrational spectra in the first step. By use of these geometries, vertical excitations will be calculated by means of several methods (TDDFT, RI-CC2, and ZINDO/S). TDDFT and RI-CC2 optimizations were performed in the lowest excited state as well. The RI-CC2 method, which is computationally much more demanding than the remaining methods mentioned, will be used as much as possible for reference purposes. Subsequently, the computed spectral characteristics will be compared with available experimental measurements for indenofluorene and/or *p*-phenylene oligomers obtained in solution and polymer matrix. The last feature of the present investigation is the extrapolation to infinite chain length in order to obtain the polymer excitation and fluorescence energy limits.

2. Computational Details

The ground state and the lowest singlet excited-state geometries of the fluorene-based oligomers were optimized at the ab initio RI-CC2[23,24] and at the DFT and TDDFT,[21,26,27] levels, respectively, using the B3LYP functional.[28] The frequencies and normal modes were determined by diagonalizing the mass-weighted force constant matrix. Geometry optimizations were restricted to C_{2v} symmetry. On the basis of the optimized geometries, the electronic absorption and luminescence spectra were calculated at the RI-CC2, TDDFT, and the ZINDO/S[29] levels. Vertical excitations are computed at the ground-state geometry. The fluorescence transition is obtained as the vertical de-excitation at the optimized geometry of the excited state. For the ZINDO/S calculations, the single excitations from the 15 highest-occupied to the 15 lowest-unoccupied molecular orbitals (HOMOs and LUMOs, respectively) were considered. The $\sigma-\sigma$ overlap weighting factor has been adjusted to 1.280 and the $\pi-\pi$ one to 0.548[30] in order to reproduce the S_1 origin of fluorene (296 nm) measured in a supersonic jet.[31] The split-valence (SV), the polarized split-valence (SVP),[32,33] and the triple-ζ valence-polarized (TZVP)[34] basis sets have been used. In case of RI-CC2 calculations, we have also augmented the SVP basis set by a set of diffuse functions whose exponents have been obtained from the lowest s, p, and d exponents by division of a factor of 3 (denoted as SVP+). All calculations were done using the Turbomole[35] and Hyperchem (ZINDO/S calculations)[36] program packages.

TABLE 1: Optimized Geometries and Total Energies in Electronic Ground (GS) and Lowest Excited States (ES) for the Fluorene Molecule (For Numbering of Bonds, See Figure 1)[a]

	GS				ES		
	B3LYP/SVP	B3LYP/TZVP	CC2/SVP	exp	B3LYP/SVP	B3LYP/TZVP	CC2/SVP
1	1.468	1.469	1.465	1.48	1.406	1.402	1.423
2	1.415	1.407	1.414	1.41	1.472	1.452	1.437
3	1.403	1.393	1.401	1.41	1.437	1.437	1.423
4	1.398	1.386	1.397	1.40	1.382	1.377	1.410
5	1.403	1.392	1.401	1.43	1.379	1.371	1.414
6	1.405	1.395	1.404	1.38	1.412	1.417	1.419
7	1.407	1.395	1.405	1.38	1.429	1.414	1.417
1′	1.513	1.513	1.510	1.47	1.515	1.512	1.506

[a] All distances are in angstroms. Experimental data (exp) are taken from ref 10.

3. Results and Discussion

The oligomer structures and the atomic numbering scheme are depicted in Figure 1. Optimized fluorene bond lengths are collected in Table 1. For the sake of comparison, the experimental X-ray data[10] are included as well. In the ground state, the B3LYP/TZVP distances are slightly shorter (about 0.006 Å) than the B3LYP/SVP ones. The RI-CC2 approach leads to practically the same bond distances as obtained with B3LYP/SVP. Bond distances agree very well with experimental values considering the fact that the latter have been determined in the solid state. The influence of the CH_2 linkage on the structure is

TABLE 2: Optimized Geometries for the Electronic Ground (GS) and Lowest Excited States (ES) for Fluorene-Based Oligomers (For Numbering of Bonds, See Figure 1)[a]

	4				6		8	
	GS		ES		GS	ES	GS	ES
	B3LYP/SVP	CC2/SVP	B3LYP/SVP	CC2/SVP	B3LYP/SVP	B3LYP/SVP	B3LYP/SVP	B3LYP/SVP
1	1.468	1.463	1.423	1.412	1.467	1.430	1.468	1.433
2	1.418	1.421	1.445	1.450	1.418	1.439	1.418	1.436
3	1.404	1.406	1.431	1.436	1.404	1.426	1.404	1.423
4	1.393	1.397	1.377	1.383	1.392	1.378	1.392	1.380
5	1.393	1.397	1.378	1.384	1.393	1.379	1.393	1.380
6	1.403	1.406	1.425	1.429	1.404	1.423	1.405	1.421
7	1.417	1.421	1.440	1.442	1.418	1.436	1.418	1.435
8	1.470	1.465	1.438	1.434	1.468	1.436	1.467	1.437
9	1.414	1.416	1.429	1.429	1.418	1.435	1.418	1.433
10	1.401	1.404	1.416	1.417	1.403	1.420	1.404	1.419
11	1.393	1.398	1.387	1.393	1.392	1.383	1.392	1.383
12	1.399	1.402	1.394	1.399	1.393	1.383	1.392	1.382
13	1.403	1.405	1.410	1.411	1.403	1.415	1.405	1.416
14	1.402	1.407	1.408	1.411	1.417	1.428	1.418	1.430
15					1.470	1.453	1.468	1.447
16					1.414	1.422	1.418	1.428
17					1.401	1.407	1.404	1.413
18					1.393	1.390	1.392	1.387
19					1.399	1.397	1.393	1.388
20					1.403	1.406	1.403	1.410
21					1.402	1.405	1.417	1.423
22							1.469	1.460
23							1.414	1.418
24							1.400	1.404
25							1.394	1.391
26							1.400	1.398
27							1.403	1.403
28							1.402	1.404
1′	1.516	1.512	1.518	1.512	1.516	1.517	1.516	1.516
2′	1.517	1.513	1.518	1.514	1.516	1.517	1.516	1.516
3′	1.515	1.513	1.516	1.514	1.516	1.517	1.516	1.516
4′					1.517	1.517	1.516	1.516
5′					1.516	1.516	1.516	1.516
6′							1.517	1.517
7′							1.518	1.517

[a] All distances are in angstroms.

illustrated by comparison of the fluorene geometry with *p*-biphenyl data.[37] In the latter case the dihedral angle between the phenylene rings is about 41°. The presence of the CH_2 bridge leads to a shortening of bonds 1 and 2 by about 0.01 Å and of the outer bonds 6 and 7 by about 0.006 Å.

The elongation of the molecular chain leads to only small changes in the inter-ring distances (see bond nos. 1, 8, 15, and 22 in Table 2) and to a slight increase in the bond length alternation (cf. neighboring intraring bond pairs 2/4, 3/5, etc.) in comparison to the fluorene molecule. The largest change occurs for a terminal ring becoming an inner one. After further extension, the bond-length differences seem to by quite well converged.

The electronic excitation leads to formation of a quinoide-type structure. The bonds 1, 4, 5, 8, 11, and 12 are shortened, while bonds 2, 3, 6, 7, 9, and 10 are elongated. The calculations at DFT/SVP and TZVP theoretical levels show the changes in distances at about 0.04 Å. The C−CH_2 bond lengths (see bonds 1′, 2′, etc.) are not affected by increasing the molecular size and by electronic excitation (see Table 2) showing that these bonds are not involved in the conjugated π system. These qualitative trends are also reflected by the RI-CC2/SVP approach (cf. ground-state and excited-state results for fluorene and the $N = 4$ case in Tables 1 and 2).

A. Vibrational Spectra. The vibrational spectrum of fluorene has attracted interest for many years. Theoretical studies on the vibrations of fluorene were presented by Lee and Boo[20] who also gave an improved vibrational assignment originally performed by Bree and Zwarich.[12] The fluorene molecule possesses 63 fundamentals. The infrared-allowed transitions belong to either a_1, b_1, or b_2 irreducible representation, while Raman allowed transitions are not restricted by symmetry. The complete set of computed vibrational frequencies and intensities are collected in Table 1S of the Supporting Information (see the end of the text for more information). The calculated vibrational spectrum (B3LYP/TZVP, scaling factor 0.9630[38]) starts at a frequency of 93 cm^{-1} (b_1 symmetry), corresponding to the out-of-plane (oop, CCC) mode coupled with the CH_2 rocking motion (see Figure 2). A very intensive peak is located at 723 cm^{-1} (experimental value 736 cm^{-1})[39] corresponding to CH oop vibrations (b_1 symmetry). Most of the modes with b_2 symmetry include torsional vibrations of the CH_2 fragment and oop CH and CCC bending (see peaks at 616, 1398, and 1433 cm^{-1}). The H-stretching vibrations of a_1 or b_2 symmetry are located at about 3000 cm^{-1}. The results calculated at the B3-LYP/SVP theoretical level very well reflect the results obtained using the TZVP basis set (see also Table 1S) as well as the DFT theoretical results published by Lee and Boo.[20] The scaled ab initio RI-CC2/SVP results (scaling factor 0.9630) show slightly overestimated C−H stretch frequencies (see Figure 2). Finally, we note that our theoretical results very well agree with the experimental observations for the gas phase.

The extension of the fluorene chain changes the position of several peaks and their intensities (see Figure 3). In comparison with fluorene, new peaks occur in the infrared spectrum, which separate the motions on inner and outer aromatic rings. For example, the band at 728 cm^{-1} corresponds to the oop CH vibrations of inner phenylene rings, while the peaks at 848 cm^{-1} are connected with motion of outer phenylene rings. The relative intensities of the peaks for outer/inner vibrations systematically increase with increasing molecular size (see arrow markers in Figure 3). The sensitivity of these vibrations on the polymerization degree was demonstrated experimentally by Athouel et al.[16] for *p*-oligophenylene thin films. Our calculations also predict small changes in peak position for C−C vibrations between 1171 and 1182 cm^{-1} and larger changes in corresponding intensities. For symmetric and asymmetric CH_2 stretches (see two peaks in the vicinity of 2900 cm^{-1} in Figure 3), changes in intensities can be observed as well.

B. Absorption and Fluorescence Transitions. The range of the lowest excitation energy in the oligomer series extends between 4.46 and 2.88 eV at the B3LYP/TZVP level (see Table 3). The next higher vertical excitations are also collected in Tables 3 and 2S. The 1^1B_2 state (HOMO−LUMO excitation) is always the lowest excited state. The next higher one is of the same symmetry for $N = 2$ and 4 but is of A_1 symmetry for all systems $N > 4$. All excitation energies decrease with the elongation of aromatic chain and display quite well a linear dependence on the inverse number of repeat units ($1/N$) (see Figure 4). For example, the addition of two phenylene rings to fluorene leads to a decrease in the excitation energy of the 1^1B_2 state of about 0.9 eV. Because of the adjustment of overlap factors (see Computational details), the semiempirical ZINDO/S results are in very good agreement with the experimental ones ($N = 2$ and 4 in Table 3).[40,41] For the fluorene molecule, the TDDFT method overestimates the excitation energies in comparison to the experimental data. The TZVP basis gives a value of 4.46 eV, which is, however, closer to experiment than the energy of 4.77 eV obtained previously using the DFT/B3LYP/6-31G method.[17] For $N > 4$, no spectroscopic data for the

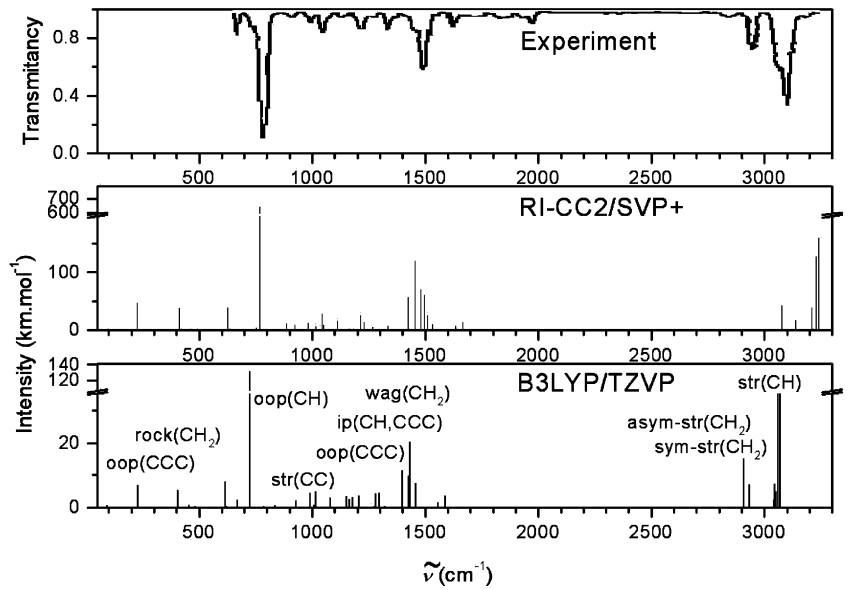

Figure 2. Calculated (B3LYP/TZVP and RI-CC2/SVP) and experimental[12] infrared spectra of fluorene ($N = 2$) in the electronic ground state. Scaling factor for theoretical frequencies was 0.9630.

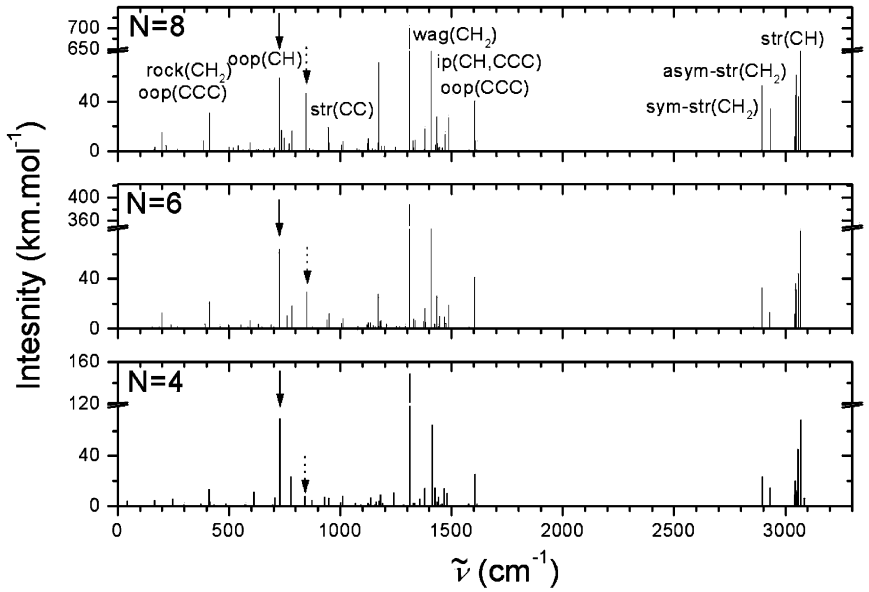

Figure 3. Calculated B3LYP/SVP infrared spectra of fluorene oligomers ($N = 4$, 6, and 8) in the electronic ground state. Scaling factor was 0.9630. The arrows denote the oop(CH) vibrations of inner (solid) and outer (dotted) phenylene rings.

fluorene-type oligomers are available. As a comparison of the oligopheneylene film, data with the available fluorene results shows (see Table 3) agreement is quite good between these two cases. The origin of this good correspondence might be explained by the increase of the electronic delocalization caused by the planarization of phenylene chains in the polymer film.[1,2] It seems that the planarization of phenylene chains using CH_2 linkages or solid state (film) environment have similar effects. Because of this finding, we decided to use experimental data for oligophenyle films[42] as the experimental reference for fluorene based oligomers ($N > 4$). On the other hand, the solution data for *p*-oligophenylenes, which are also given in Table 3, deviate considerably from the film results. The RI-CC2 calculations in SV and SVP basis sets give excitation energies, which are significantly higher than the experimental energies (see Table 2S). The extension of SVP to SVP+ leads to realistic RI-CC2 excitation energies. In all cases, the RI-CC2 results are in good accord with ZINDO/S and experimental data available for planarized oligophenylnes films.[42] The TDDFT data show a significant underestimation of the excitation energies for the larger oligomers what is in agreement with recently published theoretical results. [43,44]

The asymptotic values (extrapolated to the infinite system) are collected in the last rows of Table 3 (see also Table 2S). The calculated ZINDO/S and RI-CC2/SVP+ limits are in good agreement with the experimental value of 2.95 eV for thin films. As observed above, TDDFT underestimates and RI-CC2/SV overestimates this energy. From the dependence of the excitation energies with $1/N$, the effective conjugation length (ECL) can be deduced. This quantity represents the repeat unit number at which saturation of a property occurs and gives very useful information for the development of synthetic strategies. If we take 0.01 eV as the convergence threshold of the excitation energy with chain length, the ECL limits estimated by ZINDO/S and RI-CC2/SVP+ are 13. For B3-LYP/TZVP and RI-CC2/SV, a value of 14 is obtained. For the sake of comparison, we

TABLE 3: Theoretical and Experimental[a] Excitation and Fluorescence Energies of Oligomers Investigated and Their Polymer Limits[b]

molecule	state	TD-DFT/TZVP	RI-CC2/SVP+	ZINDO/S	exp 1	exp 2	exp 3
$N = 2$	Excitation						
	1^1B_2	4.46 (0.149)	4.57 (0.084)	4.08 (0.112)	4.14	4.08	4.92
	2^1B_2	4.64 (0.284)	5.11 (0.495)	3.89 (0.137)			
	2^1A_1	4.79 (0.007)	4.87 (0.004)	3.77 (0.000)			
	Fluorescence						
	1^1B_2	4.06 (0.461 *3.0*)	4.29 (0.138 *9.1*)	3.76 (0.675 *2.3*)	3.96	3.67	3.94
$N = 4$	Excitation						
	1^1B_2	3.49 (1.416)	3.80 (1.264)	3.53 (1.471)	3.44	3.54	4.11
	2^1B_2	3.95 (0.004)	4.25 (0.574)	3.89 (0.137)			
	2^1A_1	4.19 (0.003)	4.35 (0.003)	3.96 (0.001)			
	Fluorescence						
	1^1B_2	3.13 (1.571 *1.5*)	3.48 (1.691 *1.1*)	3.15 (1.730 *1.5*)		2.96	3.36
$N = 6$	Excitation						
	1^1B_2	3.08 (2.363)	3.47 (2.632)	3.31 (2.448)		3.27	3.98
	2^1A_1	3.67 (0.000)	4.01 (0.000)	3.75 (0.000)			
	2^1B_2	3.76 (0.003)	4.04 (0.460)	3.91 (0.088)			
	Fluorescence						
	1^1B_2	2.76 (2.559 *1.2*)	3.14 (2.974 *0.8*)	2.95 (2.569 *1.0*)		2.79	3.30
$N = 8$	Excitation						
	1^1B_2	2.88 (3.228)	3.31 (3.884)	3.20 (3.382)		3.19	3.91
	2^1A_1	3.37 (0.000)	3.77 (0.000)	3.58 (0.000)			
	2^1B_2	3.84 (0.001)	3.98 (0.482)	3.83 (0.000)			
	Fluorescence						
$N \rightarrow \infty$	1^1B_2	2.58 (3.434 *1.0*)	3.00 (4.145 *0.6*)	2.88 (3.363 *0.8*)		2.73	3.27
Excit.	1^1B_2	2.40 ± 0.05	2.92 ± 0.04	2.85 ± 0.01		2.95 ± 0.03	3.51 ± 0.08
Fluoresc.	1^1B_2	2.11 ± 0.04	2.58 ± 0.03	2.57 ± 0.01		2.47 ± 0.06	2.99 ± 0.08

[a] From experiment 1 of refs 40 and 41. [b] Energies are in eV. Values in parentheses denote oscillator strengths and fluorescence lifetimes in ns (italic). Geometries were obtained at the B3LYP/SVP level. Experiments 2 and 3 denote the experimental data for the *p*-oligophenylene series measured in film and solution,[42] respectively.

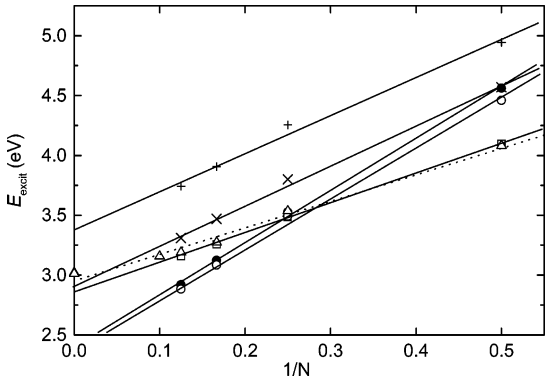

Figure 4. Dependence of the vertical excitation energy to the lowest excited state (1^1B_2) on the number of phenylene rings (*N*): TDDFT/SVP (solid circles); TDDFT/TZVP (open circles); RI-CC2/SVP (plus symbols); RI-CC2/SVP+ (× symbols); ZINDO/S (open square; and the experimental data for in thin films (open up triangles).[42] B3-LYP/SVP geometries were used.

note that the estimated ECL value for a chemically similar system poly(2,7-fluorene-*alt*-co-5,7-dihydrodibenz[c,e]oxepin) was found to be somewhat shorter with about 8 units (B3LYP/6-31G).[17]

To characterize the optical transitions, it is useful to examine HOMOs and LUMOs. The HOMO and LUMO of bifluorene ($N = 2$) and the oligomer for $N = 8$ are shown in Figure 5. Additionally, the composition of the electronic wave functions is given in Table 4. The analysis of the orbital excitations (see Table 4) indicates that the origin of the 1^1B_2 excitation in fluorene is different from the rest of the series investigated. The HOMO−LUMO excitation plays a dominant role in the larger systems, whereas in fluorene it contributes with less than 50%. It is interesting to note that in the larger molecular chains the HOMO and LUMO orbitals are localized in the central part of the molecule (see Figure 5b) whereas the HOMO − 1 and LUMO + 1 and LUMO + 2 orbitals (not shown) have strong contributions close to the oligomer edge. The LUMO orbitals nicely show the inter-ring bonding character, which is also reflected in the shortenings of the corresponding inter-ring CC distances in the excited states as discussed above.

On the basis of the geometries optimized for the first excited state, the fluorescence spectra were calculated. Figure 6 and Tables 3 and 2S illustrate the dependence of the fluorescence energies on the number of aromatic units. Similarly, as in the case of excitation energies, the theoretical asymptotic ZINDO/S and RI−CC2 results are in good agreement with the value measured for the polyphenylene film (2.47 ± 0.06 eV) in contrast to the solvent value (2.99 ± 0.08 eV).[42] The asymptotic TDDFT/TZVP value is lower about by 0.3 eV than the polyphenylene film value.

On the basis of the fluorescence energy and oscillator strength, the radiative lifetimes have been computed for spontaneous emission by using the Einstein transition probabilities according to the formula (in au)[45]

$$\tau = \frac{c^3}{2(E_{\mathrm{Flu}})^2 f} \qquad (1)$$

where c is the velocity of light, E_{Flu} is the transition energy, and f is the oscillator strength. The computed lifetime τ for the fluorene molecule (see Tables 3 and 2S) varies quite strongly between the ZINDO/S (2.3 ns), B3LYP/TZVP (3.0 ns), and RI-CC2/SVP (18.8 ns) methods. These large differences can be traced back to differences in the character of the electronic states for $N = 2$. Agreement is significantly improved for $N > 2$ (see Tables 3 and 2s). The value of 9.1 ns (RI-CC2/ SVP+) shows agreement within realistic expectations since the experimentally observed lifetime is 10 ns.[46] The increase of the molecular chain leads to a decrease of excitation energies and to an increase of oscillator strengths (see Tables 3 and 2S). This causes a decrease

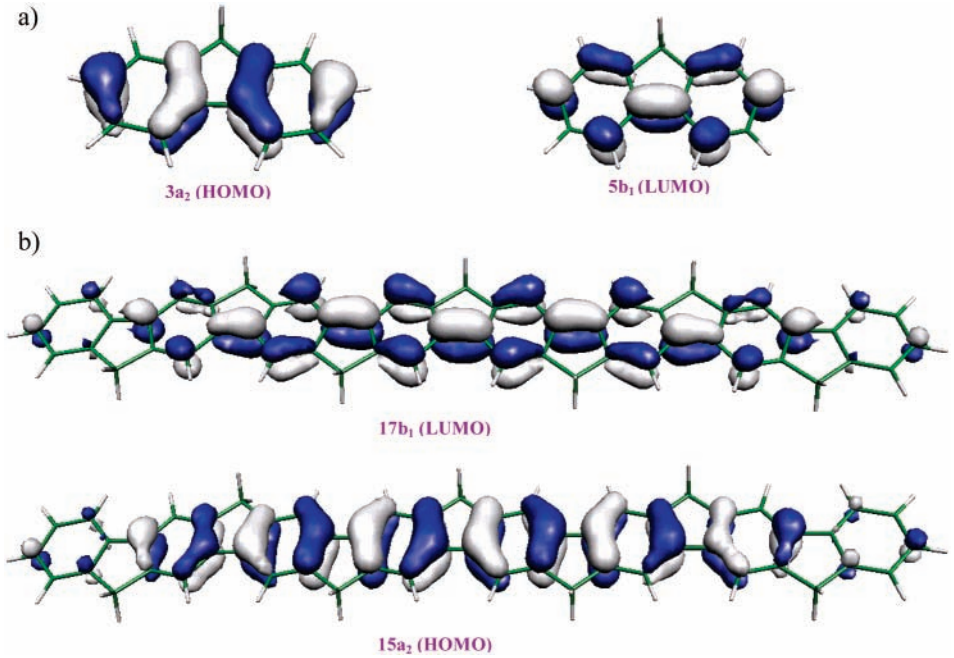

Figure 5. Plots of HOMO and LUMO (calculated at the B3-LYP/SVP level) of oligomers with (a) $N = 2$ and (b) $N = 8$.

TABLE 4: Dominant Orbital Contributions for the Lowest Three Excitations for $N = 2$ and 8 in B3-LYP/SVP Geometries[a]

molecule	B3-LYP/SVP		RI-CC2/SVP+	
$N = 2$	1^1B_2	$3a_2 \rightarrow 6b_1$ (44.2)	1^1B_2	$3a_2 \rightarrow 5b_1$ (40.7)
		$3a_2 \rightarrow 5b_1$ (37.0)		$3a_2 \rightarrow 7b_1$ (26.0)
		$2a_2 \rightarrow 5b_1$ (14.3)		$2a_2 \rightarrow 6b_1$ (13.6)
	2^1B_2	$3a_2 \rightarrow 5b_1$ (56.6)	2^1A_1	$4b_1 \rightarrow 6b_1$ (35.5)
		$3a_2 \rightarrow 6b_1$ (36.9)		$3a_2 \rightarrow 4a_2$ (28.6)
				$4b_1 \rightarrow 5b_1$ (14.2)
	2^1A_1	$4b_1 \rightarrow 5b_1$ (62.7)	2^1B_2	$3a_2 \rightarrow 6b_1$ (69.2)
		$3a_2 \rightarrow 4a_2$ (33.4)		$3a_2 \rightarrow 7b_1$ (16.1)
$N = 8$	1^1B_2	$15a_2 \rightarrow 17b_1$ (97.1)	1^1B_2	$15a_2 \rightarrow 17b_1$ (79.0)
				$16_1 \rightarrow 16a_2$ (8.1)
	2^1A_1	$15a_2 \rightarrow 16a_2$ (59.1)	2^1A_1	$15a_2 \rightarrow 16a_2$ (38.0)
		$16b_1 \rightarrow 17b_1$ (38.7)		$16b_1 \rightarrow 17b_1$ (34.6)
	2^1B_2	$15a_2 \rightarrow 19b_1$ (82.8)	2^1B_2	$15a_2 \rightarrow 18b_1$ (40.8)
		$16b_1 \rightarrow 17a_2$ (3.4)		$15a_2 \rightarrow 23b_1$ (21.3)
		$15a_2 \rightarrow 20b_1$ (3.2)		$15a_2 \rightarrow 24b_1$ (8.5)

[a] The values in parentheses stand for the excitation contributions in percentages involved in each calculated transition.

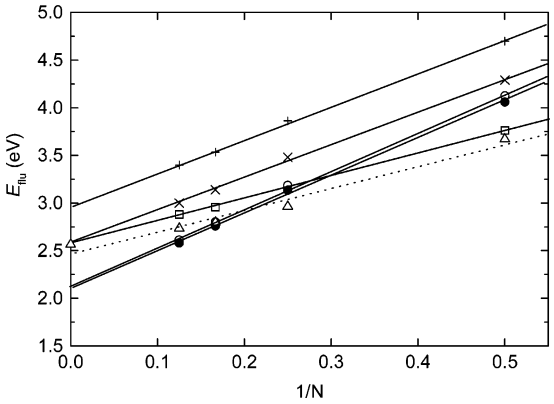

Figure 6. The dependence of the fluorescence energies on the number of phenylene rings (N): TDDFT/SVP (solid circles); TDDFT/TZVP (open circles); RI-CC2/SV (plus symbols); RI-CC2/SVP+ ($\times$ symbols); ZINDO/S (open square); and the experimental data for para oligophenylenes measured in thin films (open up triangles).[42] B3-LYP/SVP geometries were used.

of calculated radiative lifetime, e.g., RI-CC2/SVP+, results are 1.1 ns for $N = 4$, 0.8 ns for $N = 6$, and 0.6 ns for $N = 8$. Similar trends in the decrease of lifetimes were observed for unsubstituted *p*-oligophenylenes. The experimental values measured in cyclohexane solution are 16 ns for $N = 2$, 0.85 ns for $N = 4$, and 0.78 ns for $N = 6$.[14]

4. Conclusions

A systematic theoretical study has been performed on fluorene-based oligomers starting from two up to eight repeat units. Optimized geometries were obtained not only for the electronic ground state but also for the first electronically excited state. Because of computational efficiency, B3LYP has been used for the geometry optimizations of the larger oligomers. However, the RI-CC2 method could be used for extensive benchmark calculations both for geometry effects and excitation energies. ZINDO/S calculations have been performed as well using B3LYP optimized geometries. In the ground state, the RI-CC2 approach leads to a slight shortening of the inter-ring bonds and to an increase of outer bonds in comparison to DFT. Increase of the molecular size has a minimal effect on structural parameters in the ground state. The infrared spectrum for the fluorene molecule agrees very well with available experimental data. Characteristic changes with chain length of oop CH belonging to inner and to outer phenylene rings have been discussed.

Electronic excitation leads to quinoide-type distortions, in particular to a shortening of the inter-ring bonds. This behavior correlates very well with the nodal properties of the LUMO orbital. The $C-CH_2$ bond lengths are not affected by the electronic excitations. The calculated ZINDO/S electronic and fluorescence spectra are in a very good agreement with available experimental results for fluorene oligomers and with results obtained for *p*-oligophenylenes films. Inclusion of diffuse functions leads to a good description of excitation energies by the RI-CC2 method as well. On the other hand, TDDFT calculations systematically underestimate excitation and fluorescence energies for larger systems ($N > 4$) in comparison with the above-mentioned results. Good linear dependence of excita-

tion and fluorescence energies was observed with respect to $1/N$. The effective conjugation length was estimated to 13−14 repeat units. The computed radiative lifetime for the fluorene molecule is in good agreement with the experimentally observed lifetime. The decrease of the radiative lifetime with increase in conjugation length has been computed also and found to be in good agreement with experiment.

Acknowledgment. The authors acknowledge support by the Austrian Science Fund within the framework of the Special Research Program F16 and Project P14817-N03. The calculations were performed in part on the Schrödinger II cluster of the University of Vienna. This work was also supported by the Slovak Scientific Grant Agency (Project No. 1/0055/03).

Supporting Information Available: Total electronic energies, zero-point vibrational energies, optimized Cartesian coordinates for studied systems, vibrational frequencies and their intensities for the fluorene molecule, and TDDFT/SVP, RI-CC2/SV, and RI-CC2/SVP excitation and fluorescence energies. This material is available free of charge via the Internet at http://pubs.acs.org.

References and Notes

(1) Prasad, P. N.; Williams, D. J. *Introduction to Nonlinear Optical Effects In Molecules and Polymers*; John Wiley: New York, 1991.
(2) André, J. M.; Delhalle, J.; Brédas, J. L. *Quantum Chemistry Aided Design of Organic Polymers. An Introduction to the Quantum Chemsitry of Polymers and its Applications*; World Scientific: Singapore, 1991.
(3) Mabbs, R.; Nijegorodov, N. I.; Downey, W. S. *Spectrochim. Acta, A* **2003**, *59*, 1329.
(4) Nijegorodov, N. I.; Downey, W. S.; Danailov, M. B. *Spectrochim. Acta, A* **2000**, *56*, 783.
(5) Bäuerle, P. In *Electronic Materials: The Oligomer Approach*; Müllen, K., Wegner, G., Eds.; Wiley-VCH: Weinheim, New York, 1998.
(6) Johansson, N.; Salbeck, J.; Bauer, J.; Weissörtel, F.; Bröms, P.; Andresson, A.; Salaneck, W. R. *Synth. Met*. **1999**, *101*, 405.
(7) Salbeck, J.; Yu, N.; Bauer, J.; Weissörtel, F.; Bestgen, H. *Synth. Met.* **1997**, *91*, 209.
(8) Zojer, E.; Pogantsch, A.; Hennebicq, E.; Beljonne, D.; Brédas, J.-L.; List, E. J. W. *J. Chem. Phys.* **2002**, *117*, 6794.
(9) Szczepanski, J.; Banisaukas, J.; Vala, M.; Hirata, S.; Wiley, W. R. *J. Phys. Chem. A* **2002**, *106*, 6935.
(10) Burns, D. M.; Iball, J. *Proc. R. Soc. (London)* **1955**, *A227*, 200.
(11) Boo, B. H.; Choi, Y. S.; Kim, T. S.; Kang, S. K.; Kang, Y. H.; Lee, S. Y. *J. Mol. Struct.* **1996**, *377*, 129.
(12) Bree, A.; Zwarich, R. *J. Chem. Phys.* **1969**, *51*, 903.
(13) Nijegorodov, N. I.; Downey, W. S. *J. Phys. Chem.* **1994**, *98*, 5639.
(14) Nijegorodov, N. I.; Mabbs, R. *Spectrochim. Acta, A* **2000**, *56*, 2157.
(15) Thormann, T.; Rogojerov, M.; Jordanov, B.; Thulstrup, E. W. *J. Mol. Struct.* **1999**, *509*, 93.
(16) Athouel, L.; Wéry, J.; Dulieu, B.; Bullot, J.; Buisson, J. P.; Froyer, G. *Synth. Met.* **1997**, *84*, 287.
(17) Wang, J. F.; Feng, J.-K.; Ren, A.-M.; Liu, X.-D.; Ma, Y.-G.; Lu, P.; Zhang, H.-X. *Macromolecules* **2004**, *37*, 3451.
(18) Zojer, E.; Pogantsch, A.; Hennebicq, E.; Beljonne, D.; Brédas, J.-L.; List, E. J. W. *J. Chem. Phys.* **2002**, *117*, 6794.
(19) Beljonne, D.; Pourtois, G.; Shuai, Z.; Hennebicq, E.; Scholes, G. D.; Brédas, J. L. *Synt. Met.* **2003**, *137*, 1369.
(20) Lee, S. Y.; Boo, B. H. *J. Phys. Chem.* **1996**, *100*, 8782.
(21) Furche, F.; Ahlrichs, R.; *J. Chem. Phys*. **2002**, *117*, 7433.
(22) Christiansen, O.; Koch, H.; Jørgensen, P. *Chem. Phys. Lett*. **1995**, *243*, 409.
(23) Köhn, A.; Hättig, C. *J. Chem. Phys*. **2003**, *119*, 5021.
(24) Hättig, C. *J. Chem. Phys*. **2003**, *118*, 7751.
(25) Aquino, A. J. A.; Lischka, H.; Hättig, Ch. *J. Phys. Chem. A*, in press.
(26) Bauernschmitt, R.; Ahlrichs R. *Chem. Phys. Lett.* **1996**, *256*, 454.
(27) Bauernschmitt, R:, Häser, M:, Treutler; O., Ahlrichs R. *Chem. Phys. Lett.* **1997**, *264*, 573.
(28) Becke, A. D. *J. Chem. Phys*. **1993**, *98*, 5648.
(29) Zerner, M. C.; Loew, G. H.; Kirchner, R. F.; Mueller-Westerhoff, U. T. *J. Am. Chem. Soc.* **1980**, *102*, 589.
(30) Belletête, M.; Morin, J. F.; Beaupré, S.; Leclerc, M.; Durocher, G. *Synth. Met.* **2002**, *126*, 43.
(31) Zhang, X.; Pitts, J. D.; Nadarajah, R.; Knee, J. L. *J. Chem. Phys.* **1997**, *107*, 8239.
(32) Dunning, T. H.; Harrison P. J. In *Modern Theoretical Chemistry*; Shaefer, H. F., III, Ed.; Plenum Press: New York, 1977; Vol. 2.
(33) Dunning, T. H.; Hay, P. J. In *Methods of electronic structure Theory*; Schaefer H. F., III, Ed.; Plenum Press: New York, 1977; Vol. 2.
(34) Godbout, N.; Salahub, R.; Andzelm, J.; Wimmer, E. *Can. J. Chem.* **1992**, *70*, 560.
(35) Ahlrichs, R.; Bär, M.; Häser, M.; Horn, H.; Kölmel, C. *Chem. Phys. Lett.* **1989**, *162*, 165.
(36) HYPERCHEM, rel. 7.5 for Windows, Hypercube, Inc. 2003.
(37) Grein, F. *THEOCHEM* **2003**, *623*, 23 and references therein.
(38) Rauhut, G.; Pulay; P. *J. Phys. Chem.* **1995**, *99*, 3093.
(39) NIST Mass Spec Data Center. Infrared Spectra. In *NIST Chemistry WebBook, NIST Standard Reference Database Number 69*; Linstrom, P. J., Mallard, W. G., Eds.; March 2003, National Institute of Standards and Technology, Gaithersburg MD, 20899; http://webbook.nist.gov.
(40) Ramart-Lucas, M.; Matti, M. J.; Guilmart, T. *Bull. Soc. Chim. Fr.* **1948**, *15*, 1215.
(41) Stauner, T.; Avar, L.; Chardonnens, L. *Helv. Chim. Acta* **1970**, *53*, 1311.
(42) Matsuoka, S.; Fuji, H.; Yamada, T.; Pac, C.; Ishida, A.; Takamuku, S.; Kusaba, M.; Nakashima, N.; Yanagada, S.; Hashimoto, K.; Sakata, T. *J. Phys. Chem.* **1991**, *95*, 1991.
(43) Dierksen, M.; Grimme, S. *J. Phys. Chem. A.* **2004**, *108*, 10225.
(44) Belletête, M.; Durocher, G.; Hamel, S.; Côte, M.; Wakim, S.; Leclerc, M. *J. Chem. Phys.* **2005**, *122*, 104303.
(45) Litani-Barzilai, I.; Bulatov, V.; Schechter, I. *Anal. Chim. Acta* **2004**, *501*, 151.